Interannual variability in the wintertime air–sea flux of carbon dioxide in the northern North Atlantic, 1981–2001

Are Olsen[a, b], Richard G. J. Bellerby[b, a], Truls Johannessen[a, b], Abdirahman M. Omar[b, a] and Ingunn Skjelvan[a, b]

[a] Geophysical Institute, University of Bergen, Allégaten 70, 5007, Bergen, Norway
[b] Bjerknes Centre for Climate Research, University of Bergen, Allégaten 55, 5007, Bergen, Norway

Abstract

Gridded fields of sea surface temperature (SST), sea level pressure (SLP), and wind speed were used in combination with data for the atmospheric mole fraction of CO_2 and an empirical relationship between measured values of the fugacity of carbon dioxide in surface water and SST, to calculate the air–sea CO_2 flux in the northern North Atlantic. The flux was calculated for each of the months October–March, in the time period 1981 until 2001, allowing for an assessment of the interannual variations in the region. Locally and on a monthly time scale, the interannual variability of the flux could be as high as ±100% in regions seasonally covered by sea ice. However, in open-ocean areas the variability was normally between ±20% and ±40%. The interannual variability was found to be approximately halved when fluxes averaged over each winter season were compared. Summarised over the whole northern North Atlantic, the air to sea carbon flux over winter totalled 0.08 Gton, with an interannual variability of about ±7%. On a monthly basis the interannual variations were slightly higher, about ±8% to ±13%. Changes in wind speed and atmospheric fCO_2 (the latter directly related to SLP variations) accounted for most of the interannual variations of the computed air–sea CO_2 fluxes. A tendency for increasing CO_2 flux into the ocean with increasing values of the NAO index was identified.

Author Keywords: North Atlantic; Nordic Seas; Carbon fluxes; Air–sea interaction; Interannual variability; North Atlantic Oscillation; 45–80°N; 45°W–20°E

1. Introduction

Because of its ability to retain outgoing long wave radiation, CO_2 in the atmosphere acts as a greenhouse gas serving to modify the global radiation budget, and its atmospheric concentration is considered to play a major role in global climate regulation. This has been substantiated by the observation of decreased levels of atmospheric CO_2 during ice ages, as deduced from ice core data (e.g. [Petit et al (1999)]). Since the industrial revolution, the atmospheric CO_2 levels have increased from ~280 ppm to the present day levels of ~370 ppm ([Keeling and Whorf (2001)]) because of emissions of anthropogenic CO_2. The elevated levels of atmospheric CO_2 are cause for concern as they may have adverse effects on climate ([IPCC (2001)]).

Presently, approximately half of the anthropogenic CO_2 release remains in the atmosphere; the rest is distributed between the terrestrial biosphere and the oceans ([Marland and Boden (2001)]). The relative sizes and the locations of these sinks are a matter of debate (e.g. [Fan et al (1998)]; [Guerney et al (2002)]). Determination of

the ocean uptake of atmospheric carbon dioxide is often carried out by determination of the concentration gradient between the atmosphere and the ocean, which in combination with wind speed data allows for calculation of the air–sea flux of CO_2 (e.g. [Liss and Merlivat (1986)]). However, because of natural climate variability the air–sea flux of CO_2 may vary considerably from one year to another (e.g. [Skjelvan et al (1999)]; [Louanchi and Hoppema (2000)]), implying that measurements from several years are necessary to accurately constrain the long-term flux.

The northern North Atlantic is considered to be an important sink region for CO_2, because of the large heat loss and convective processes taking place there. There is a substantial large-scale climatic variability in this area, which is described by the North Atlantic Oscillation (NAO) index ([Hurrell (1995)]), a measure of the distribution of atmospheric mass over the region. The NAO index is defined as the difference between the normalised surface pressure at a northern (usually Stykkisholmur, Iceland) and a southern (usually Ponta Delgada, Portugal) station, and alternates between positive and negative states, reflecting a dipole pattern in the pressure field over the region. A positive NAO state is associated with an intensified Icelandic low-pressure cell and an anomalously strong Azores high-pressure cell. This leads to a northward shift of the westward storm track over the North Atlantic, as compared to the conditions during negative NAO states when the pressure anomaly pattern is approximately reversed. Furthermore, during positive NAO states the Norwegian Atlantic Current, a northward extension of the North Atlantic Current, appears to narrow, whilst the polar water from the Arctic extends more to the east ([Blindheim et al (2000)]; [Furevik (2001)]). Given the imprint of the NAO on both the atmospheric and oceanic conditions, there is a need to assess its impact on the air–sea flux of CO_2 in the northern North Atlantic. Such an assessment is especially relevant in light of the conclusion reached by [Bates and Merlivat (2001)], who found that: "Interannual variations of atmospheric forcing in response to modes of climatic variability should also play a significant role in determining interannual variability in the global ocean uptake of CO_2". However, because there is no long-term time series data of CO_2 system parameters in the region, this issue has not as yet—to the best of our knowledge—been very extensively addressed in the scientific literature. The present work seeks to fill this gap by using an empirical relationship between the fugacity of CO_2 in surface water (fCO_2^{sw}) and sea surface temperature (SST) to extrapolate available measurements of fCO_2^{sw} in both time and space. Its application is based on the assumption that as fCO_2^{sw} is changed by processes such as mixing, biological activity, and gas exchange it will change in correspondence with the SST ([Stephens et al (1995)]; [Lee et al (1998)]). The technique has been employed in several regions to estimate the large-scale CO_2 flux ([Stephens et al (1995)]; [Goyet et al (1998)]; [Hood et al (1999)]) and its interannual variability ([Lee et al (1998)]). In the current work, the method is applied to the northern North Atlantic, aiming to acquire an estimate of the interannual variability of the air–sea CO_2 flux. Furthermore, as the NAO might lock into a positive phase in a global warming scenario ([Skjelvan et al (1999)]), the results may indicate the direction of change the CO_2 flux in this region may experience in the future.

The present study concentrates on the winter season, defined here as October to March, as fCO_2^{sw} was found to be decoupled from SST during the rest of the year, using available data. The time period was set by the record of gridded temperature fields available, which cover the period from November 1981 until present ([Reynolds and Smith (1994)]).

2. Data and procedures

The present study is confined to the area north of the North Atlantic Gyre, excluding shelf areas (shallower than 200–500 m). The southern boundary was set at 45°N; the eastern boundary was set at 10°W up to 50°N, then followed the continental shelf edge northwards to 80°N. Finally, the western boundary was set at the east Greenland continental shelf edge, or the ice edge when this had a more eastward extension, southwards from 80° N to Cape Farewell—the southern tip of Greenland—and at that longitude down to 45°N.

SST and fCO_2^{sw} data were obtained from various sources as listed in Table 1. The tracks of the expeditions are

depicted in Fig. 1.

Table 1. Sources of fCO_2^{sw} data

Platform	Time	Area	Originator
R/V *Hudson*	February–March 1982	NA/GIN	R. Weiss
R/V *Polarstern*	March 1993	GIN	B. Schneider
R/V *Håkon Mosby*	February–March 1995	GIN	I. Skjelvan/T. Johannessen
R/V *Håkon Mosby*	November 1995	GIN	I. Skjelvan/T. Johannessen
R/V *Knorr*	November 1996	NA	R. Wanninkhof
Carioca buoy	Winter 1996/1997	GIN	L. Merlivat/M. Hood
R/V *Håkon Mosby*	February–March 1997	GIN	A.M. Omar/T. Johannessen
R/V *Knorr*	October–November 1997	NA	R. Wanninkhof
R/V *Håkon Mosby*	March 1998	GIN	A.M Omar/T. Johannessen

Areas are NA: North Atlantic; GIN: Greenland–Iceland–Norwegian Seas.

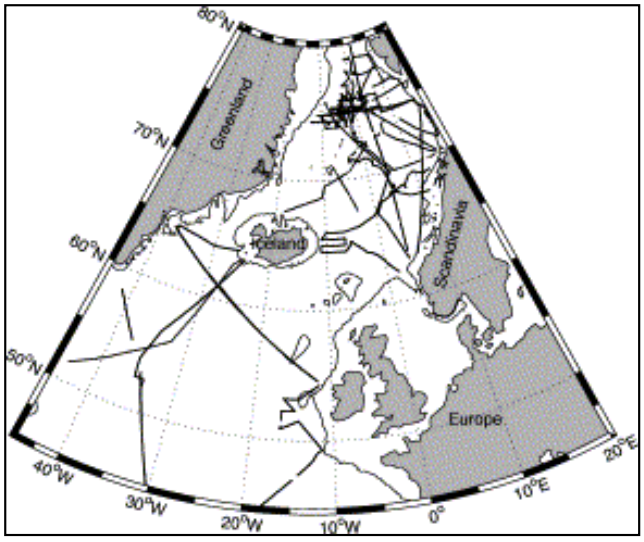

Fig. 1. Northern North Atlantic fCO_2^{sw} data acquired during winter (October–March) 1982–1998. The thin line marks the position of the 300 m isobath, serving as an indication of the continental shelf areas that were excluded from this study. South of Greenland, the western boundary was set at the longitude of Cape Farewell. South of 50°N, the eastern boundary was set at 10°W.

Data acquired at temperatures lower than −1.8°C were excluded from the data set as this is the cut off point of the temperature fields ([Reynolds and Smith (1994)]), which were employed to calculate the fCO_2^{sw} fields.

2.1. Adjustment of fCO_2^{sw} data to the year 1995

The fCO_2^{sw} data were acquired between 1982 and 1998 (Table 1) which is almost the whole time period covered by the present study. The atmospheric CO_2 concentration measured at Barrow, Alaska (71°N), increased by approximately 1.4 ppm yr^{-1} ([Keeling and Whorf (2001)]) over this time interval.

The response of surface seawater fCO_2 in the northern North Atlantic to the atmospheric fCO_2 increase is not known. [Takahashi et al (1995)] assume that the anthropogenic signal in fCO_2^{sw} in this region is diluted by open-ocean convective mixing. However, this assumption is based on observations obtained at Ocean Weather Station

P, which is located in the northwestern subarctic Pacific. At least four recent observations in northern North Atlantic indicate that fCO_2^{sw} here increases at the same rate as fCO_2^{atm} or at a faster rate. Firstly, the anthropogenic carbon transport calculation carried out by [Rosón et al (2003)] indicates that the region north of 24.5°N is a small source of anthropogenic CO_2, which implies that fCO_2^{sw} increases at a slightly higher rate than fCO_2^{atm}. Secondly, [Omar et al (1967)] have compared fCO_2^{sw} data obtained in the Barents Sea, i.e. in the northernmost extensions of the North Atlantic Current, in 2000/2001 with data obtained by [Kelley (1970)] in 1967. Accounting for variations in the natural controls of the ocean CO_2 system, their results show that the surface ocean fCO_2 in the Barents Sea has tracked the atmospheric increase over the last 33 years. Thirdly, [Lefèvre et al. (submitted)] have analysed the evolution of monthly detrended ΔfCO_2 in the North Atlantic subpolar gyre (50–80°N, 80°W–20°E) over the time period 1981–1998. Accounting for temperature effects their analysis, which includes the data that we have used, shows an apparent decrease in the air–sea fCO_2 gradient over the last two decades of ~0.4 μatm yr^{-1}. And, fourthly, using a conceptual advective model [Anderson and Olsen (2002)] find that the region north of 50°N in the North Atlantic Ocean is likely a source of anthropogenic CO_2, which also implies that fCO_2^{sw} increases at a higher rate than fCO_2^{atm} in this region.

The data used in the present paper have also been checked for any long-term trend in surface ocean fCO_2. This was carried out by comparing the mean of the fCO_2 data from the 1982 Hudson cruise with the mean of the fCO_2 data from the other cruises (covering the time span 1993–1998, see Table 1). For comparison, selection of 1982 data was limited to those measurements which lay within a distance of 2°×2° from any of the 1993–1998 data and vice versa. The fCO_2 values were normalised to 5°C according to the iso-chemical temperature dependency of [Takahashi et al (1993)], $\delta \ln fCO_2/\delta T$=4.23% $°C^{-1}$, in order to account for temperature effects. The mean of the 1982 data was 332 μatm, whereas the mean of the 1993–1998 data was 367 μatm. This rough analysis also indicates an increase in northern North Atlantic surface ocean fCO_2.

In light of these results, it would perhaps be natural to assume that northern North Atlantic surface ocean fCO_2 has increased at a greater rate than the atmospheric fCO_2. However, considering the uncertainty of the quoted findings, the relatively small decrease of the air–sea gradient, and the potential but completely unknown interannual variations of this decrease, we assume in the following that northern North Atlantic surface seawater fCO_2 tracks the atmospheric fCO_2 increase.

Thus, any interannual variability of fCO_2^{sw} is assumed to be superimposed on a steady increase tracking that of the atmosphere, which implies that there is no anthropogenic component in the interannual variability of ΔfCO_2. It is therefore possible to use the atmospheric level from one year when estimating the air–sea fluxes in the present study, provided the fCO_2^{sw} fields are calculated from a fCO_2^{sw}–SST relationship that reflects the conditions during the same year. Hence, to allow the 1995 level of atmospheric CO_2 to be used in the flux calculations, measured fCO_2^{sw} data were normalised to the year 1995 creating $fCO_{2\text{–}95}^{sw}$, by assuming an increase of 1.4 μatm yr^{-1}.

2.2. Calculation of monthly $fCO_{2\text{–}95}^{sw}$ fields

The $fCO_{2\text{–}95}^{sw}$ data were normalised to 5°C according to [Takahashi et al (1993)], in order to remove the thermodynamic effect on fCO_2^{sw}. By this operation the variable henceforth referred to as $fCO_{2\text{–}95}^{sw}$ was obtained.

The relationship between $fCO_{2\text{–}95}^{sw}$ and SST is depicted in Fig. 2. Despite the substantial spatial and temporal

spread of the source data, the relation falls close to a straight line with a slope of −11.2 (r^2=0.96), which is consistent with the findings of [Hood et al (1999)] in the Greenland Sea. However, some nonlinearity was evident and a cubic relation found by least squares regression gave an improved fit:

$$fCO_{2-95N}^{sw}=391.13-8.71SST-0.36SST^2+0.011SST^3 \quad [n=15154,\ r^2=0.97]. \qquad (1)$$

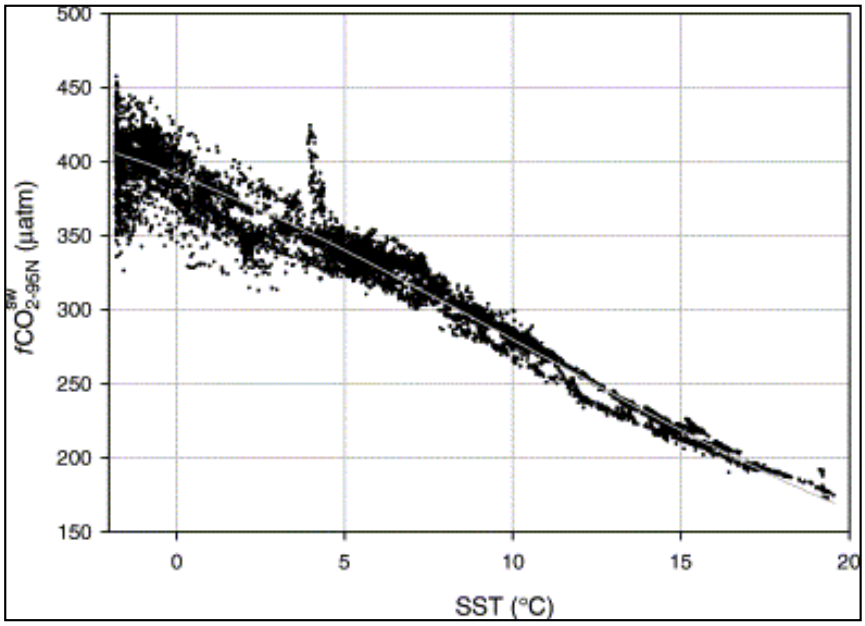

Fig. 2. Relationship between fCO_{2-95}^{sw} and SST. The grey line shows the cubic fit to the data.

The scatter around the estimated regression line increases at temperatures below 5°C. For one thing this reflects the larger amount of data at low temperatures, but it also highlights the dynamical nature of the northern areas where these data were acquired. We identify likely processes to be: events of intense heat loss causing decreasing temperatures with the following gas exchange occurring at different rates; ice edge upwelling; and influence of high-alkalinity Arctic Waters. However, the spatial and temporal extent of these processes appear limited as the long-term and large-scale trend is strong over the whole range of SSTs. Excluding groups of data that were substantially offset from the regression line did not change the fit to any significant extent.

Monthly fields of fCO_{2-95}^{sw} were calculated by applying Eq. (1) on monthly fields of SST with a 1°×1° resolution. The SST fields were derived from ship, buoy, and bias corrected satellite data by the [Reynolds and Smith (1994)] analysis, and were obtained from the IRI/LDEO Climate Data Library at http://ingrid.ldgo.columbia.edu/. Fields of fCO_{2-95}^{sw} were converted to the in situ temperature according to [Takahashi et al (1993)], giving monthly fields of fCO_{2-95}^{sw}.

The calculations yield a set of 119 fields of the monthly distribution of fCO_2^{sw} normalised to the year 1995. The fields cover the winter months October through March, in the time period November 1981 until March 2001. These fields were used in the calculation of the air–sea CO_2 flux fields to be described in Section 2.4.

2.3. Validation of monthly fCO_{2-95}^{sw} fields

The computed fields were compared with the measured fCO_2^{sw} data. This was carried out by first bin averaging the measured fCO_2^{sw} values normalised to 1995 into boxes of size 1°×1°×month, i.e. the same grid resolution as the fields estimated above. The difference between the computed and bin averaged value in each of the boxes containing any measurements was then calculated. Latitudinally averaged differences and their standard deviations are depicted in Fig. 3. Evidently, the estimated fields reproduce the large-scale fCO_{2-95}^{sw} distribution quite well, as the offset is generally within ±10 μatm. There is however a substantial increase in both the offset and the spread north of 70°N. At 71.5°N, this is due to the group of data that is completely decoupled from SST at ~4°C, left unexplained in the paper describing these ([Hood et al (1999)]). Furthermore, the increased variability over the whole region north of 70°N is due to data from close to the ice edge, illustrating that a simple fCO_2^{sw}–SST relationship fails to reproduce the fCO_2^{sw} distribution in such regions.

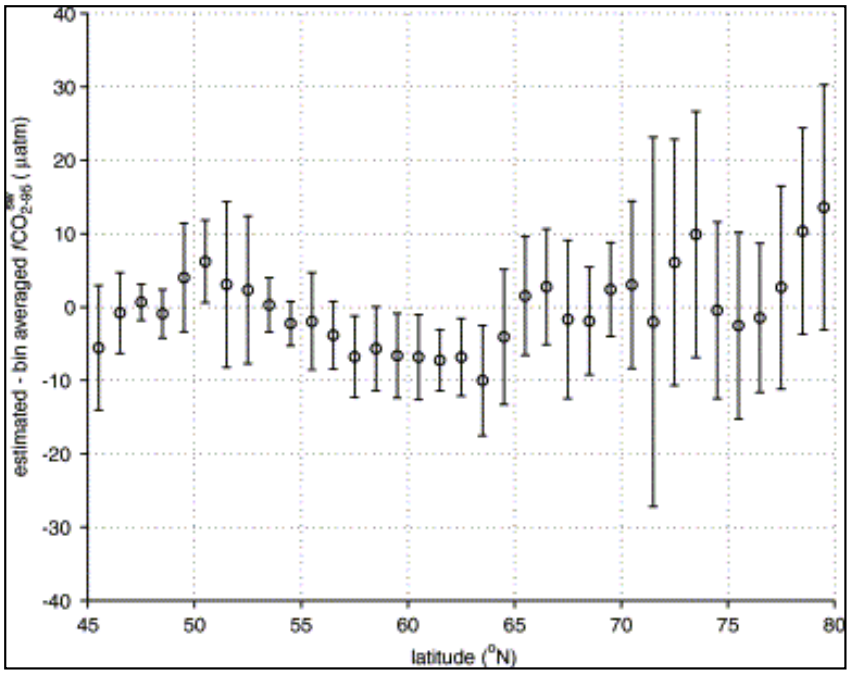

Fig. 3. Difference between measured fCO_2^{sw} values, normalised to 1995 and bin averaged into boxes of size 1°×1°×month, and values estimated from Eq. (1). The differences have been averaged along each latitude. The error bars are the standard deviation for each average value.

2.4. Calculation of monthly air–sea CO_2 flux maps

The air–sea flux was calculated according to

$$F = K_0 k (fCO_2^{atm} - fCO_2^{sw}), \quad (2)$$

where K_0 is the solubility, k is the transfer velocity for air–sea CO_2 exchange, and fCO_2^{sw} and fCO_2^{atm} are the sea surface and atmospheric fCO_2. Solubility was calculated according to [Weiss (1974)], from the same SST fields that were employed to compute the fCO_{2-95}^{sw} fields. The transfer velocity was calculated from the [Wanninkhof (1992)] relationship for long-term averaged winds and monthly fields of wind speed at 10 m above the sea surface. The monthly wind speed fields were computed from fields of

six hourly wind vectors from the NCEP/NCAR reanalysis project ([Kalnay et al (1996)]). The reanalysis data were provided by the NOAA-CIRES Climate Diagnostics Center, Boulder, CO, USA, from their web site at http://www.cdc.noaa.gov/. These data were supplied on an approximately 2.5°×2.5° grid, and were regridded by a triangle-based cubic spline interpolation to fit the 1°×1° grid of the fCO_{2-95}^{sw} fields.

Data for the atmospheric mole fraction of CO_2 (XCO_2) were made available by the NOAA, CMDL Carbon Cycle Group flask sampling programme. Monthly mean values from Zeppelin Mountain, Spitsbergen (79°N); Ocean Weather Station M, Norwegian Sea (66°N); Mace Head, Ireland (53°N); and the Azores (39°N), for each of the winter months (January–March and October–December) in 1995, were linearly regressed to obtain the latitudinal gradient of XCO_2 in the study area. The regression coefficients are presented in Table 2. Longitudinal variations in XCO_2 are assumed to be negligible. The pCO_2^{atm} in each grid point was then calculated according to

$$pCO_2^{atm}=XCO_2(p_b-pH_2O), \quad (3)$$

where p_b is the barometric pressure, and pH_2O is the water vapour pressure calculated from SST according to [Cooper et al (1998)]. Gridded fields of sea level pressure (SLP) were used for p_b. These were obtained from the NOAA-CIRES Climate Diagnostics Center, Boulder, CO, USA, from their web site at http://www.cdc.noaa.gov/, and originate from the NCEP/NCAR reanalysis project ([Kalnay et al (1996)]). The SLP data were supplied on an approximately 2.5°×2.5° grid and were regridded by a triangle-based cubic spline interpolation to fit the 1°×1° grid of the fCO_{2-95}^{sw} fields. pCO_2^{atm} were converted to fCO_2^{atm} by assuming a 0.3% decrease from the pCO_2^{atm} value ([Weiss (1974)]), a procedure considered sufficiently accurate for the present purpose.

Table 2. Regression coefficients for the line XCO_2=a×latitude+b, describing the latitudinal gradient of the atmospheric CO_2 mole fraction over the northern North Atlantic in 1995

Month	*a*	*b*	r^2
October	0.019	357.1	0.17
November	0.045	359.5	0.70
December	0.041	361.9	0.75
January	0.074	358.4	0.78
February	0.098	358.0	0.94
March	0.107	358.4	0.99

The flux in ice covered regions was set to zero. These were identified by having a SST of −1.8°C following [Reynolds and Smith (1994)].

The calculations yielded monthly fields of the air–sea CO_2 flux, over the winter months October–March from November 1981 until March 2001.

3. Results

The maximum fCO_{2-95}^{sw} values are found between approximately 50°N and 60°N (Fig. 4, Fig. 5 and Fig. 6a). The values decrease moving northwards and westwards, reflecting the distribution of the warm North Atlantic Water. The decreasing fCO_{2-95}^{sw} values at the southern limit of the study area, moving into the North Atlantic Gyre, are in

accordance with the findings of [Takahashi et al (1995)]. There is little change in the fCO_{2-95}^{sw} fields between November and February (Fig. 4a vs. Fig. 5a), a slight increase in the southern parts and a slight decrease in the Norwegian Atlantic Current reflecting colder temperatures. The estimated interannual variability in fCO_{2-95}^{sw} is small and generally less than ±1%, ~3 μatm (Fig. 4, Fig. 5 and Fig. 6c). The flux fields (Fig. 4, Fig. 5 and Fig. 6b) show that the most intense sink is in the Greenland Sea, where the air–sea CO_2 flux is on the order of 10–20 mmol m^{-2} d^{-1}. Close to the ice edge the values drop, because of the averaging of values from years when the area was ice covered (i.e. no flux) and ice free. The weakest sink area is south of Iceland, where the flux ranges from below 2 up to 4 mmol m^{-2} d^{-1}. This is because of low fCO_2^{atm} values in that region as is evident from Fig. 7, which shows as an example the mean distribution of fCO_2^{atm} in February. The present study covers a time period when the NAO was almost always in a positive phase, characterised by an intense Icelandic low-pressure cell which leads to low atmospheric partial pressures of CO_2 (through Eq. (3)), ultimately giving rise to the modest air–sea CO_2 flux that we observe in that region. In the North Atlantic Current system, the flux ranges from about 2 to 6 mmol m^{-2} d^{-1}, and to the south, in the North Atlantic Gyre, the flux is on the order of 4–8 mmol m^{-2} d^{-1}. The mean air–sea flux is higher in February than in November. This seasonal signal is mainly a result of higher atmospheric concentrations of CO_2 in February than in November (Table 2).

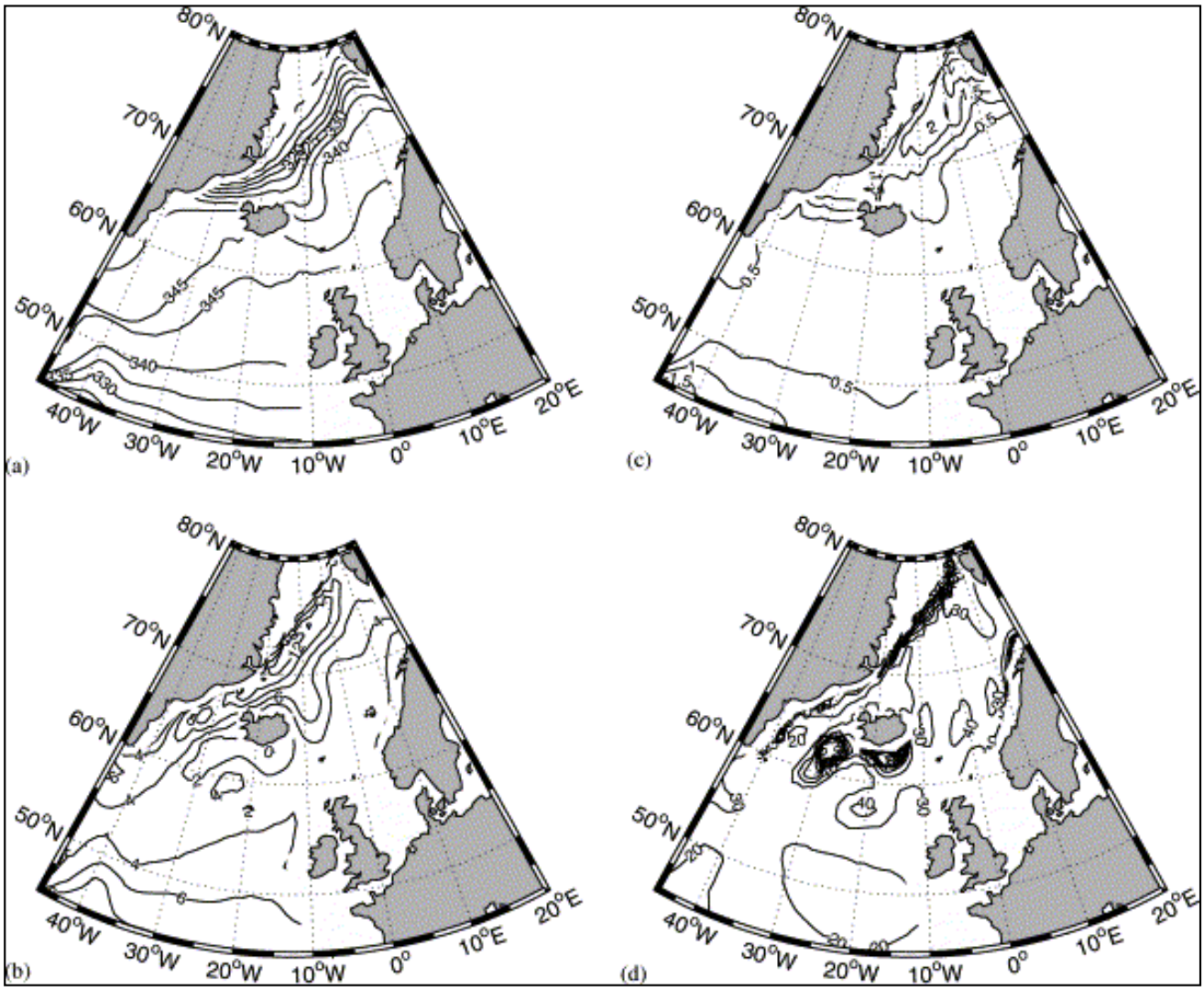

Fig. 4. (a,b) Mean distribution of fCO_{2-95}^{sw} (in μatm) and air–sea CO_2 flux (in mmol m^{-2} d^{-1}) in November. (c,d) Interannual standard deviation of fCO_{2-95}^{sw} and air–sea CO_2 flux in November, expressed as per cent of the mean value. The dashed line is the mean ice border in November, defined after [Reynolds and Smith (1994)].

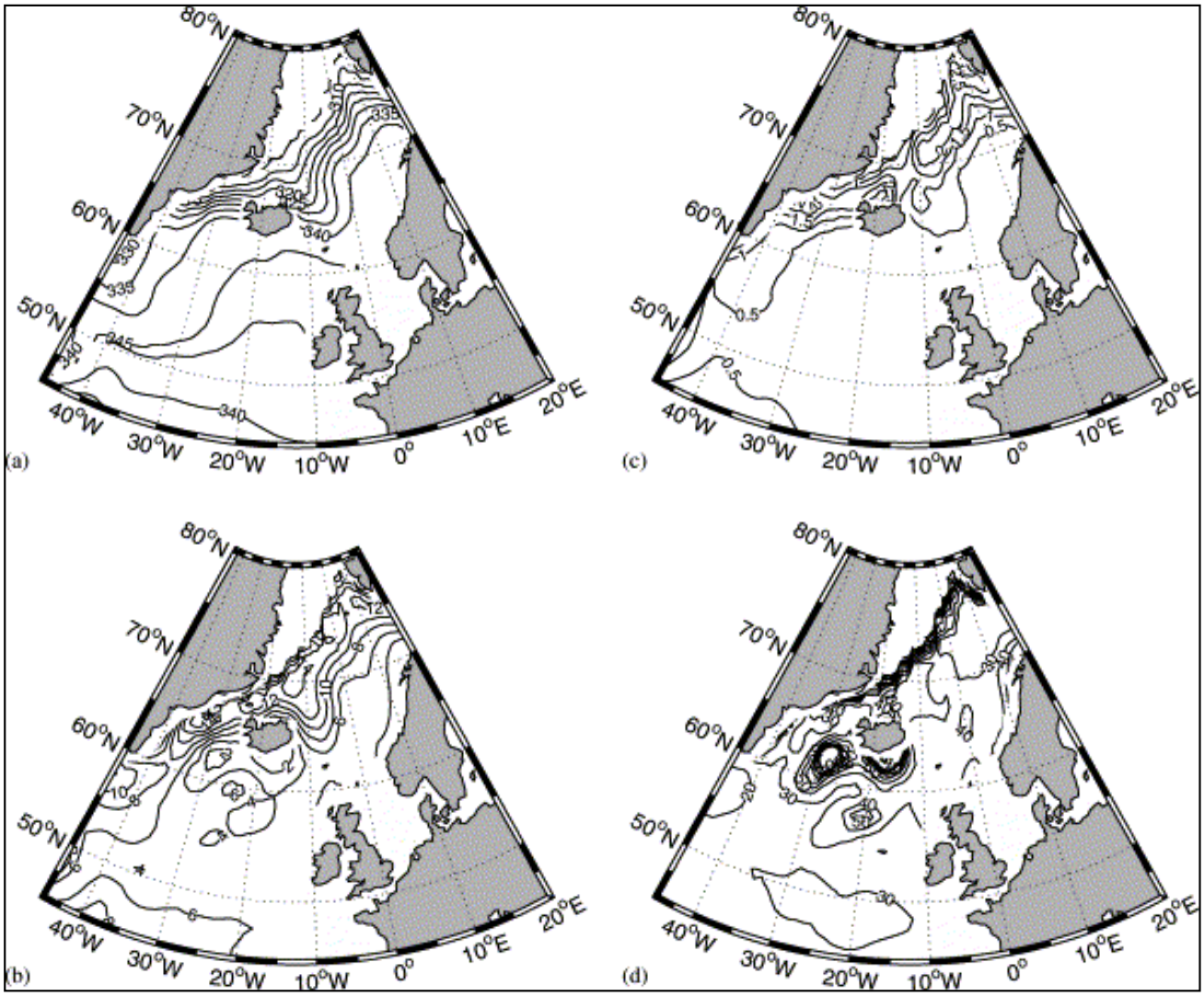

Fig. 5. Same as Fig. 4, but for the month of February.

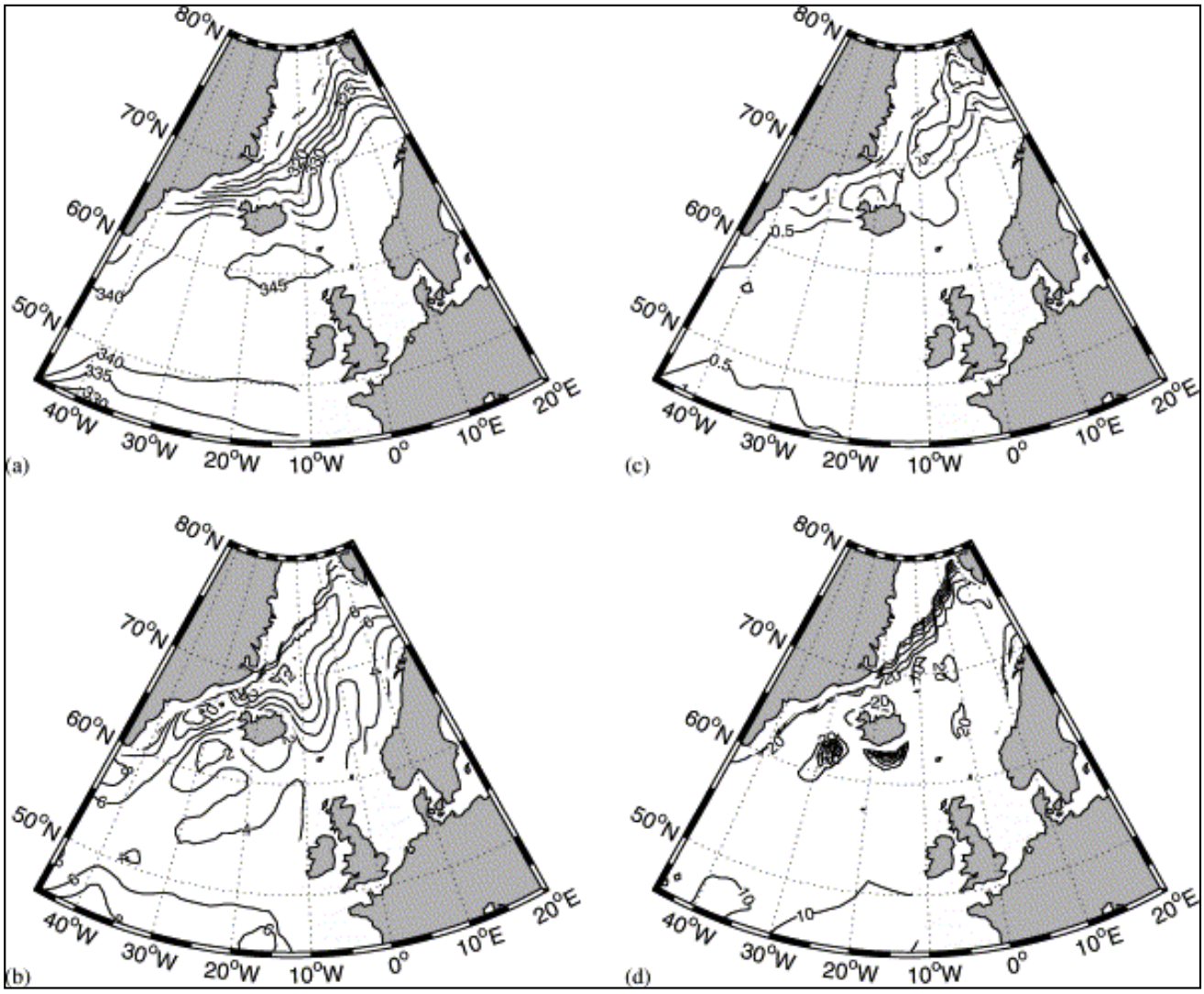

Fig. 6. Same as Fig. 4, but for the winter season.

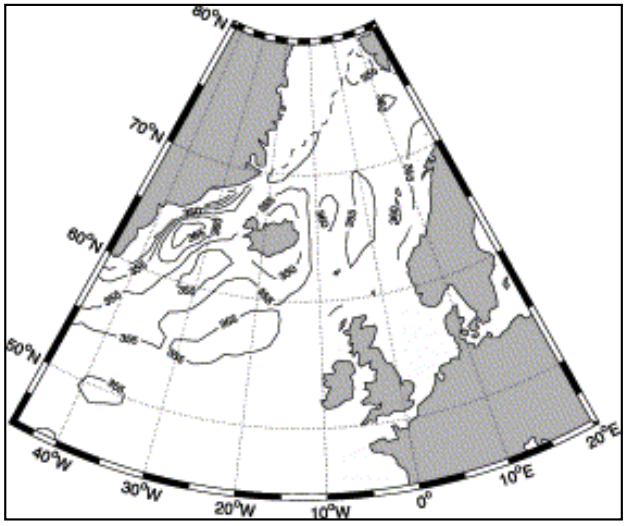

Fig. 7. Mean distribution of fCO_2^{atm} (in μatm) in February.

The interannual variability of the monthly air–sea CO_2 flux (Fig. 4 and Fig. 5) is substantial over the whole area in both February and November. The variability is largest close to the ice edge, reaching ±100%, and is due to interannual differences in areal sea ice extent. There are also substantial variations in the Irminger Sea and to the east, south of Iceland. The air–sea CO_2 flux is rather low in this region; therefore, even small changes will result in a large relative variability, which is what we present in our figures. Further south and in the North Atlantic Current system the

interannual variability is in the range of ±20% to ±40%. The interannual variability appears slightly larger in February than in November. The interannual variability is in the range of ±10% to ±20% when average values from the whole winter season are considered (Fig. 6d). This shows that the variations in the individual months are partially averaged out over the winter season.

The interannual variability of the fCO_{2-95}^{sw} fields is small, and the large interannual variability in the monthly fluxes must therefore be due to the other factors that determine the flux, mainly wind speed and fCO_2^{atm}. To identify the processes that control the interannual variations of air–sea CO_2 exchange, the air–sea CO_2 flux fields and their interannual variability were computed as described above. However, this time all parameters were kept constant at their mean value in each grid point, except for either fCO_{2-95}^{sw}, fCO_2^{atm}, or wind speed which were, one at a time, allowed to vary as in the original computations. The results for the month of February are reproduced in Figs. 8(a)–(c), which show the interannual standard deviation in the air–sea CO_2 flux fields caused by variations in fCO_{2-95}^{sw}, fCO_2^{atm} or wind speed. Additionally, since both wind speed and fCO_2^{atm} depend on the SLP distribution and will tend to co-vary, the fluxes were computed varying both of these whilst holding the other parameters constant at their mean value. The result for the month of February is reproduced in Fig. 8d. The ice border was held constant at its mean value and the variability close to the ice edge is not present in these fields.

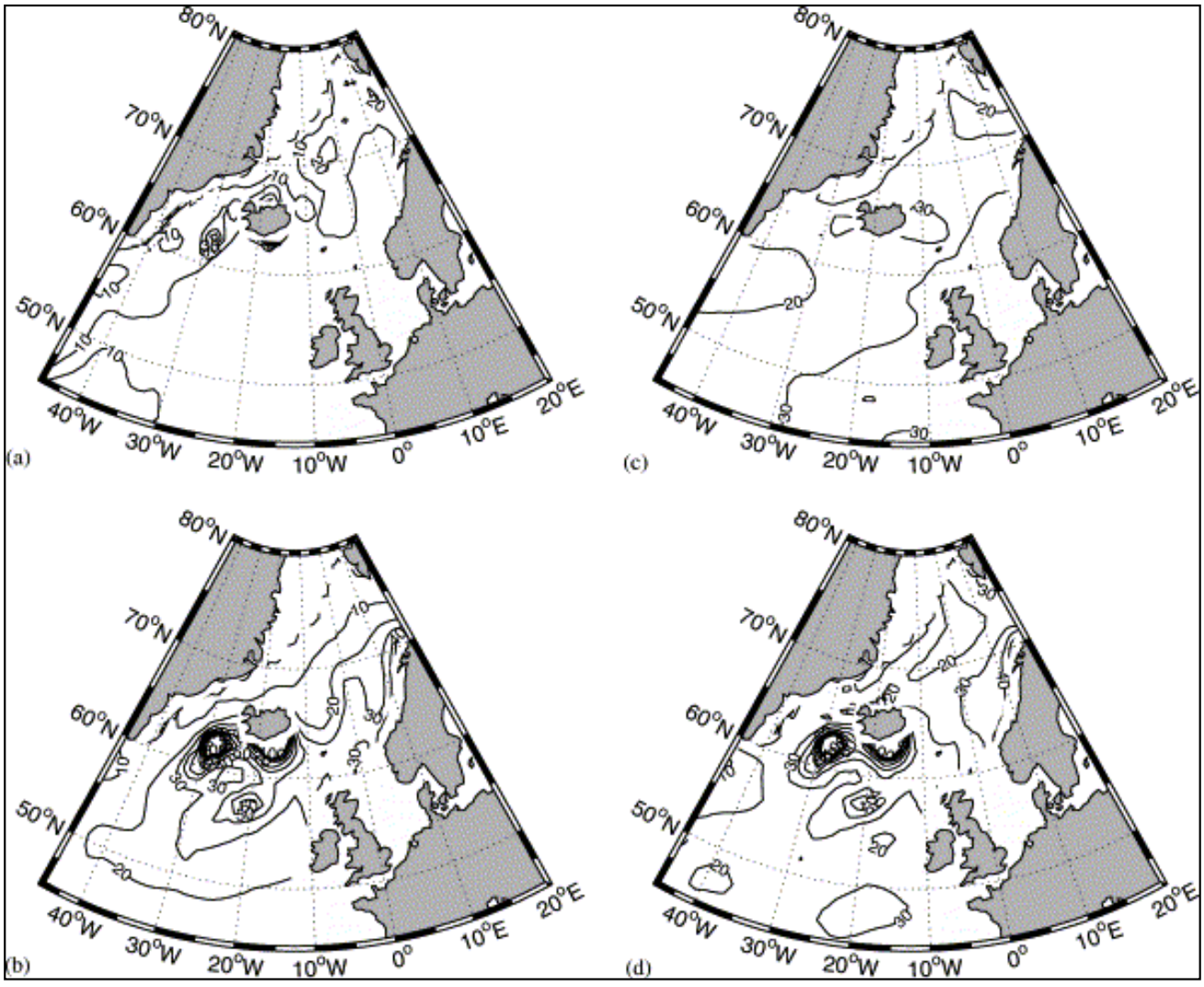

Fig. 8. Interannual standard deviation of the air–sea CO_2 flux due to fCO_{2-95}^{sw} (a), fCO_2^{atm} (b), and wind speed (c) variations in the month of February. (d) Interannual standard deviation of the flux computed when both fCO_2^{atm} and wind speed were varied. The standard deviation is expressed as per cent of the mean value.

Variations in the air–sea CO_2 flux caused by changes in fCO_{2-95}^{sw} only are generally quite small, less than ±10% (Fig.

8a). Only in the northern reaches of the study area and around Iceland does fCO_{2-95}^{sw} variability change the flux significantly, up to around ±20%, which is still less than observed when all parameters were varied simultaneously (Fig. 5d). Both fCO_2^{atm} and wind speed variations (Figs. 8b and c) can on their own give rise to air–sea CO_2 flux changes that are comparable to those observed when all parameters were varied simultaneously (Fig. 5d). But, it is only when fCO_2^{atm} and wind speed are varied simultaneously (Fig. 8d) that both the magnitude and spatial distribution of the interannual flux variations observed in Fig. 5d are reproduced. Interannual variations in the air–sea CO_2 flux in the northern North Atlantic appear thus to be controlled mainly through the combined action of fCO_2^{atm} and wind speed forcing. The only exception is just to the south of Iceland, where air–sea CO_2 flux variability appears to rely primarily on changes in fCO_2^{atm} only (Fig. 8b).

Changes in the NAO index are in essence a measure of changes in the SLP distribution and therefore wind speed over the northern North Atlantic. Positive NAO states are associated with an almost regional lowering of SLP relative to negative NAO states, with the largest depressions occurring over the Irminger Sea ([Cayan (1992)]). Furthermore, as the NAO index becomes more positive, wind speeds increase over the whole region. The most significant increase occurs south of the low-pressure centre, across the North Atlantic between 50°N and 65°N ([Cayan (1992)]), which is the southern part of the present study area. Therefore, an increase in the NAO index will on one hand act to decrease the air–sea CO_2 flux through decreased fCO_2^{atm} caused by lower SLP (Eq. (3)), whilst on the other it will act to increase the flux through increased wind speed. Thus, the correlation coefficient between the monthly NAO index as defined by [Jones et al (1997)] and the monthly flux anomaly in each grid point (Fig. 9) does not only show the extent to which the air–sea CO_2 exchange is influenced by the NAO. It also provides information, through its sign, on whether the influence is through wind speed variability or fCO_2^{atm} variations. The correlation coefficients are positive west of the British Isles between approximately 45°N and 55°N, and reach up to between 0.5 and 0.6. Here therefore, the flux of CO_2 into the ocean tends to increase as the NAO index increases, following increased surface wind speeds. Correlation coefficients are negative, reaching down to −0.4 in the Irminger Sea and to the east, south of Iceland. Here, the air–sea CO_2 flux tends to decrease as the NAO index increases. An increase in the NAO index implies decreased SLP and therefore, as fCO_2^{atm} decreases so does the air–sea CO_2 flux. Finally, in the Nordic Seas correlation coefficients are by and large quite low so the air–sea CO_2 flux in this region does not respond to changes in the state of the NAO index. The only exception is just to the north of the Denmark Strait, a region that experiences significantly higher wind speed as the NAO index increases ([Kwok and Rothrock (1999)]).

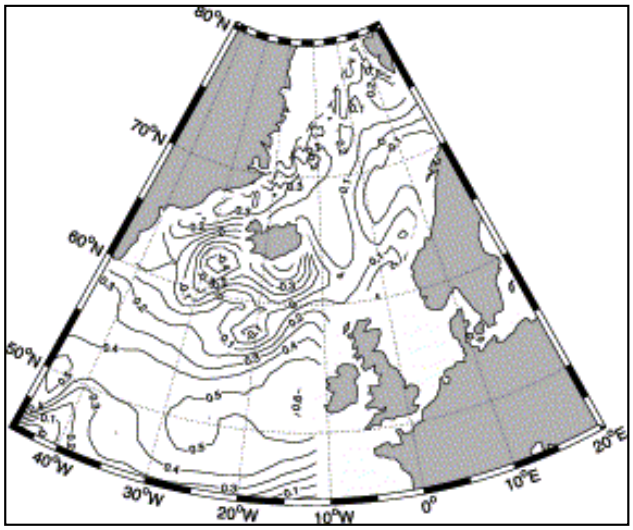

Fig. 9. Correlation coefficient (*r*) between the monthly NAO index and air–sea CO_2 flux anomaly.

Table 3 summarises the net exchange of CO_2 integrated over the region as defined in Section 2, and its interannual variability. Values are given for each month and for the whole winter season. The net uptake over winter in the region is normally around 81.9×10^{12} g C, or 0.01 Gton. Interannual variability between winters is in the range of $\pm5.5\times10^{12}$ g C, corresponding to approximately ±7%. But the difference between two winters can be up to 4 times larger, when maximum and minimum values are compared.

Table 3. Estimated air–sea CO_2 flux in 10^{12} g C in the northern North Atlantic, and its interannual variability

	October	November	December	January	February	March	Winter
Mean	9.29	12.3	15.2	14.5	15.2	15.2	81.9
S.D.	0.82	1.2	1.5	1.8	1.7	1.6	5.6
Max.	10.4	14.9	17.9	18.4	17.9	17.8	91.3
Min.	7.98	9.85	12.1	11.8	11.8	11.7	71.9

During the individual months the mean net uptake is about $9–15\times10^{12}$ g C, with an interannual variability in the range of $\pm1–2\times10^{12}$ g C or about ±8% to ±13%. The difference between 2 years can be up to 6.5×10^{12} g C when maximum and minimum values in individual months are compared.

4. Discussion

The present estimates of the air–sea CO_2 flux are comparable with previous estimates. [Hood et al (1999)] obtained a flux of about 8–16 mmol m^{-2} d^{-1} during winter season in the Greenland Sea using the [Wanninkhof (1992)] transfer velocity equation. [Skjelvan et al (1999)] estimated fluxes on the order of 20 mmol m^{-2} d^{-1} in the Greenland Sea and 6 mmol m^{-2} d^{-1} in the Norwegian Atlantic Current. The consistency between these regional estimates and our results lends confidence to our method.

Our flux estimates have not been compared with those of [Takahashi et al (2002)] because of the different schemes used to project the data onto a single year. [Takahashi et al (2002)] assume that there is no anthropogenic increase in North Atlantic fCO_2^{sw}, and applies therefore no correction when projecting fCO_2^{sw} data collected over several years onto the single year 1995. We, on the other hand, assume that fCO_2^{sw} increases at the same rate as the atmosphere, and applies this correction when projecting fCO_2^{sw} data onto 1995. Thus evidently, while the Takahashi fluxes will have a substantial anthropogenic component (see also below), ours have none, and the estimates should not be compared.

The estimated interannual variability of the air–sea CO_2 flux was dependent on the time and length scale used. The interannual variability in the whole area was estimated to be less than ±7% for the air–sea flux summarised over the winter season (Table 3), and it was slightly larger when individual months were compared, ±8% to ±13%. On the other hand, on a monthly time scale the interannual standard deviation fields revealed interannual variations up to ±100% in areas influenced by the presence of sea-ice and south of Iceland. But variations were normally in the range of ±20% to ±40%, depending on the region (Fig. 4 and Fig. 5). Additionally the fields confirm the time-scale dependence, as interannual variability decreased to between ±10% and ±20% when values averaged over the winter season (Fig. 6d) were compared. As expected, interannual variability tends to be reduced when values integrated over long time intervals and large areas are compared, and estimates of seasonal and regional interannual variability based on comparison of "snap-shot" measurements as in [Skjelvan et al (1999)] are most likely overestimates.

The interannual variations in the air–sea CO_2 flux were related mainly to variability of the atmospheric forcing parameters fCO_2^{atm} and wind speed (Fig. 8), and the interannual variability of fCO_{2-95}^{sw} as calculated from SST was only about ±1% (Fig. 4, Fig. 5 and Fig. 6c). The interannual SST changes in the region are small, about ±0.5–1°C ([Levitus et al (2000)]); therefore, any conceivable change in the slope of Eq. (1) will not change the magnitude of the interannual variations in fCO_{2-95}^{sw}.

Air–sea CO_2 exchange proved sensitive to NAO variations mainly in two regions: south of Iceland, where the flux decreases following increasing NAO index; and west of the British Isles, where the flux tends to increase as the NAO index increases. These are the regions where there is greatest association between the NAO index and the SLP and wind speed variations ([Cayan (1992)]). Some response was also evident north of the Denmark Strait, but elsewhere correlation coefficients were rather low. Thus, the atmospheric variations causing the interannual flux variations in these regions are not intimately linked with the NAO index. Nevertheless, when the air–sea CO_2 flux integrated over the whole region and over each winter were compared with the classical winter (DJFM) NAO index, a tendency for increasing CO_2 flux into the ocean with increasing NAO index was identified (2×10^{12} g C over winter per unit change of the NAO index, r=0.49, p value 0.03). Most of this positive response of the air–sea CO_2 flux to NAO index changes can be attributed to the increased uptake in the large region west of the British Isles through increased wind speeds as the NAO index increases. The highly variable region south of Iceland is of little importance because of its comparatively small area and low mean air–sea CO_2 flux.

We identify three potential sources of error that may have led us to underestimate the interannual variability of the air–sea CO_2 flux: (1) negligence of interannual variations in the atmospheric fCO_2 increase, (2) the assumption that the ocean fCO_2 increases at the same rate as the atmospheric fCO_2, and (3) potential inability of a constant SST–fCO_2 relationship to reproduce the true interannual variations of ocean fCO_2. First, the interannual variability of the atmospheric fCO_2 increase has not been considered in this work. A constant growth rate of atmospheric fCO_2 of 1.4 μatm yr^{-1} was assumed, whereas the true rate has varied between the extreme values of 0.2 and 3.2 μatm yr^{-1}, being typically between 1 and 2 μatm yr^{-1} ([CMDL (2002)]) over the time period of our calculations. The typical variation in the atmospheric growth rate is thus less than the variation in ocean fCO_2 that was computed for the open-ocean regions in the northern North Atlantic (Fig. 4, Fig. 5 and Fig. 6c). Given this, and given that the year to year changes in open-ocean fCO_2 did not generally cause any significant interannual flux variations (Fig. 8a), the use of a constant atmospheric fCO_2 growth rate has only introduced a small error in our estimate of interannual air–sea CO_2 flux variability.

Secondly, the assumption that surface ocean fCO_2 increases at the same rate as the atmospheric fCO_2 can be questioned. As was discussed in Section 2.1 the air–sea fCO_2 gradient in the region may be increasing because of upwelling of deep water that has not been exposed to the present atmosphere ([Takahashi et al (1997)]), or it may be decreasing as is indicated by model calculations ([Anderson and Olsen (2002)]) and ocean data ([Rosón et al (2003)]; [Lefèvre et al. (submitted)]). To assess the likely changes in the air–sea flux that can be induced by a steadily increasing air–sea fCO_2 gradient, the air–sea flux into the present study area was computed for an increasing atmosphere–ocean gradient of 1.4 μatm yr^{-1}, following the "full correction" assumption of [Takahashi et al (1997)]. This yielded a steady increase in the wintertime ocean uptake of 7×10^{12} g C yr^{-1}, which is slightly larger than the natural variability between winters, $\pm5.5\times10^{12}$ g C (Table 3). And of course, a decreasing air–sea fCO_2 gradient of 1.4 μatm yr^{-1}, more than three times the value found by [Lefèvre et al. (submitted)], will yield a steady decrease in the flux of 7×10^{12} g C yr^{-1}.

Thirdly as pointed out above, use of a constant relationship between $fCO_{2-95}{}^{sw}$ and SST to compute $fCO_{2-95}{}^{sw}$ fields will inevitably predict low interannual variation, because of the relatively small interannual changes of SST in the region. However, there may be interannual changes in the relationship between SST and $fCO_{2-95}{}^{sw}$ so that the use of a constant relationship over the years may have led to the underestimation of the interannual variability of $fCO_{2-95}{}^{sw}$. Changes in the SST–$fCO_{2-95}{}^{sw}$ relationship may be caused by the increased transfer of atmospheric CO_2 to the ocean in periods of persistently higher wind speeds and vice versa. Also, the assumption of correspondence between $fCO_{2-95}{}^{sw}$ and SST changes during mixing may not be valid, and interannual changes in the $fCO_{2-95}{}^{sw}$–SST relationship can be brought about by changes in the mixing depth expected from changes in wind speed. As of now, with no other data available, we take the uncertainty in the $fCO_{2-95}{}^{sw}$ fields of ±10 μatm (Section 2.3) as a measure of the maximum likely interannual

variations in the large-scale fCO_{2-95}^{sw} distribution in the area, since this uncertainty more or less reflects deviations from an estimated mean value in each grid point. Sensitivity calculations, carried out by determining the air–sea flux as a function of fCO_2^{sw} using data from selected grid points, showed that the effect of such potential variations of fCO_2^{sw} on the flux is of magnitude similar to the computed interannual flux variations. For one thing this observation highlights the need for a better assessment of marine CO_2 variability at different length and time scales to allow more robust estimates of interannual variations in the air sea CO_2 flux. But it also implies, as we would like to emphasise here, that interannual variations in atmospheric forcing are at least as important as variations in fCO_2^{sw} in determining interannual variability in the wintertime ocean uptake of CO_2 in the northern North Atlantic region. Estimates for the global oceans have shown that variability in wind forcing accounts for approximately 10% of the interannual variations in the air–sea CO_2 transfer ([Lee et al (1998)]). The present results show that there may be substantial regional deviations from this number.

Finally, we note that the atmospheric circulation over the North Atlantic may lock into a positive NAO mode following global warming ([Skjelvan et al (1999)]). Neglecting changes in water column chemistry, our results show that this will lead to enhanced wintertime air to sea CO_2 transfer into the northern North Atlantic. Additionally, the expected decrease in sea ice cover extent ([Vinnikov et al (1999)]) will also enhance the flux into the region.

Acknowledgements

This work was supported by grants from the Norwegian Research Council and the European Commission through the project CAVASSOO (EVK2-CT-2000-00088).

We would like to thank Marie Hood, Lilliane Merlivat, Bernd Schneider, and Rik Wanninkhof for allowing us to use their fCO_2^{sw} data. We are also grateful to Ludger Mintrop for building the CARINA database. The Hudson 82 ([Weiss et al (1992)]) data were obtained from the website of CDIAC at: http://cdiac.esd.ornl.gov/.

Comments from Leif G. Anderson, Ferial Louanchi and two anonymous reviewers helped improve the manuscript. This is publication No. 35 of the Bjerknes Centre for Climate Research.

References

Anderson and Olsen (2002). Anderson, L.G., Olsen, A., 2002. Air–sea flux of anthropogenic carbon dioxide in the North Atlantic. Geophysical Research Letters 29(17), 10.1029/2002GL014820.

Bates and Merlivat (2001). N.R. Bates and L. Merlivat, The influence of short-term wind variability on air–sea CO_2 exchange. *Geophysical Research Letters* **28** (2001), pp. 3281–3284.

Blindheim et al (2000). J. Blindheim, V. Borokov, B. Hansen, S.-Aa. Malmberg, W.R. Turrell and S. Østerhus, Upper layer cooling and freshening in the Norwegian Sea in relation to atmospheric forcing. *Deep-Sea Research I* **47** (2000), pp. 655–680.

Cayan (1992). D.R. Cayan, Latent and sensible heat flux anomalies over the Northern Oceans: the connection to monthly atmospheric circulation. *Journal of Climate* **5** (1992), pp. 354–369.

CMDL (2002). CMDL, 2002. CMDL summary report #26 (2000–2001). Climate Monitoring and Diagnostics Laboratory, Boulder, CO, USA, obtainable at http://www.cmdl.noaa.gov.

Cooper et al (1998). D.J. Cooper, A.J. Watson and R.J. Ling, Variation of pCO_2 along a North Atlantic shipping route (UK to the Caribbean): a year of automated observations. *Marine Chemistry* **60** (1998), pp. 147–164.

Fan et al (1998). S. Fan, M. Gloor, J. Mahlman, S. Pacala, J. Sarmiento, T. Takahashi and P. Tans, A large terrestrial carbon sink in North America implied by atmospheric and oceanic carbon dioxide data and models. *Science* **282** (1998), pp. 442–446.

Furevik (2001). T. Furevik, Annual and interannual variability of Atlantic water temperatures in the Norwegian and Barents Seas: 1980–1996. *Deep-Sea Research I* **48** (2001), pp. 383–404.

Goyet et al (1998). C. Goyet, F.J. Millero, D.W. O'Sullivan, G. Eischeid, S.J. McCue and R.G.J. Bellerby, Temporal variations of pCO_2 in surface seawater of the Arabian Sea in 1995. *Deep-Sea Research I* **45** (1998), pp. 609–623.

Guerney et al (2002). K.R. Guerney, R.M. Law, A.S. Denning, P.J. Rayner, D. Baker, P. Bousquet, L. Bruhwiler, Y.-H. Chen, P. Ciais, S. Fan, I.Y. Fung, M. Gloor, M. Heimann, K. Higuchi, J. John, T. Maki, S. Maksyutov, K. Masarie, P. Peylin, M. Prather, B.C. Pak, J. Randerson, J. Sarmiento, S. Taguchi, T. Takahashi and C.-W. Yuen, Towards robust regional estimates of CO_2 sources and sinks using atmospheric transport models. *Nature* **415** (2002), pp. 626–630.

Hood et al (1999). E.M. Hood, L. Merlivat and T. Johannessen, Variations of fCO_2 and air–sea flux of CO_2 in the Greenland Sea gyre using high-frequency time series data from CARIOCA drift buoys. *Journal of Geophysical Research* **104** (1999), pp. 20571–20583.

Hurrell (1995). J.W. Hurrell, Decadal trends in the North Atlantic Oscillation: regional temperatures and precipitation. *Science* **269** (1995), pp. 676–679.

IPCC (2001). IPCC, 2001. Climate change 2001: the scientific basis. Contribution of Working Group I to the Third Assessment Report of the Intergovernmental Panel on Climate Change. Available online at http://www.ipcc.ch/.

Jones et al (1997). P.D. Jones, T. Jonsson and D. Wheeler, Extension to the North Atlantic Oscillation using early instrumental pressure observations from Gibraltar and South-West Iceland. *International Journal of Climatology* **17** (1997), pp. 1433–1450.

Kalnay et al (1996). E. Kalnay, M. Kanamitsu, R. Kistler, W. Collins, D. Deaven, L. Gandin, M. Iredell, S. Saha, G. White, J. Woollen, Y. Zhu, M. Chelliah, W. Ebisuzaki, W. Higgins, J. Janowiak, K.C. Mo, C. Ropelewski, A. Leetmaa, R. Reynolds and R. Jenne, The NCEP/NCAR reanalysis project. *Bulletin of the American Meteorological Society* **77** (1996), pp. 437–471.

Keeling and Whorf (2001). Keeling, C.D., Whorf, T.P., 2001. Atmospheric carbon dioxide record from Mauna Loa. In: Trends Online: A Compendium of Data on Global Change. Carbon Dioxide Information Analysis Center, Oak Ridge National Laboratory, U.S. Department of Energy, TN, USA. Available online at http://cdiac.esd.ornl.gov.

Kelley (1970). J.J. Kelley, Carbon dioxide in the surface waters of the North Atlantic Ocean and the Barents and Kara Seas. *Limnology and Oceanography* **15** (1970), pp. 80–87.

Kwok and Rothrock (1999). R., Kwok and D.A. Rothrock, Variability of Fram Strait ice flux and North Atlantic Oscillation. *Journal of Geophysical Research* **104** (1999), pp. 5177–5189.

Lee et al (1998). K. Lee, R. Wanninkhof, T. Takahashi, S.C. Doney and R.A. Feely, Low interannual variability in recent oceanic uptake of atmospheric carbon dioxide. *Nature* **396** (1998), pp. 155–159.

Lefèvre et al. (submitted). Lefèvre, N., Watson, A.J., Olsen, A., Ríos, A., Pérez, F., Johannessen, T., 2003. A decrease in the sink of atmospheric CO_2 in the North Atlantic, Submitted for publication.

Levitus et al (2000). S. Levitus, C. Stephens, J. Antonov and T. Boyer, Yearly and year-season upper ocean temperature anomaly fields 1948–1998, NOAA Atlas NESDIS 40. , US Department of Commerce, Washington, DC (2000).

Liss and Merlivat (1986). P.S. Liss and L. Merlivat, Air–sea gas exchange rates: introduction and synthesis. In: P. Buat-Ménard, Editor, *The Role of Air–sea Exchange in Geochemical Cycling*, Riedel, Norwell, MA (1986), pp. 113–129.

Louanchi and Hoppema (2000). F. Louanchi and M. Hoppema, Interannual variations of the Antarctic CO_2 uptake from 1986 to 1994. *Marine Chemistry* **72** (2000), pp. 103–114.

Marland and Boden (2001). Marland, G., Boden, T., 2001. The increasing concentration of atmospheric CO_2: how much, when, and why? Presented at Erice International Seminars on Planetary Emergencies, 26th Session, Erice, Sicily, Italy, 19–24 August 2001. In: Trends Online: A Compendium of Data on Global Change, Carbon Dioxide Information Analysis Center, Oak Ridge National Laboratory, U.S. Department of Energy, TN, USA. Available online at http://cdiac.esd.ornl.gov.

Omar et al (1967). Omar, A.M., Johannessen, T., Kaltin, S., Olsen, A, 2003. The anthropogenic increase of oceanic pCO_2 in Barents Sea surface waters since 1967. Journal of Geophysical Research, in press.

Petit et al (1999). J.R. Petit, J. Jouzel, D. Raynaud, N.I. Barkov, J.-M. Barnola, I. Basile, M. Benders, J. Chappellaz, M. Davis, G. Delaygue, M. Delmotte, V.M. Kotlyakov, M. Legrand, V.Y. Lipenkov, C. Lorius, L. Pépin, C. Ritz, E. Saltzman and M. Stievenard, Climate and atmospheric history of the past 420,000 years from the Vostok ice core, Antarctica. *Nature* **399** (1999), pp. 429–436.

Reynolds and Smith (1994). R. Reynolds and T. Smith, Improved global sea surface temperature analyses. *Journal of Climate* **7** (1994), pp. 929–948.

Rosón et al (2003). Rosón, G., Rios, A., Lavín, A., Pérez, F.F., Bryden, H.L., 2003. Carbon distribution, fluxes and budgets in the subtropical North Atlantic Ocean (24.5°N). Journal of Geophysical Research 108, doi: 10.1029/1999JC000047.

Skjelvan et al (1999). D.T. Shindell, R.L. Miller, G.A. Schmidt and L. Pandolfo, Simulation of recent northern winter climate trends by greenhouse forcing. *Nature* **399** (1999), pp. 452–455.

Skjelvan et al (1999). I. Skjelvan, T. Johannessen and L.A. Miller, Interannual variability of fCO_2 in the Norwegian and Greenland Seas. *Tellus Series B* **51** (1999), pp. 477–498.

Stephens et al (1995). M.P. Stephens, G. Samuels, D.B. Olson, R.A. Fine and T. Takahashi, Sea–air flux of CO_2 in the North Pacific using shipboard and satellite data. *Journal of Geophysical Research* **100** (1995), pp. 13571–13583.

Takahashi et al (1993). T. Takahashi, J. Olafsson, J.G. Goddard, D.W. Chipman and S.C. Sutherland, Seasonal variation of CO_2 and nutrients in the high latitude surface oceans: a comparative study. *Global Biogeochemical Cycles* **7** (1993), pp. 843–878.

Takahashi et al (1995). T. Takahashi, T.T. Takahashi and S.T. Sutherland, An assessment of the role of the North Atlantic as a CO_2 sink. *Philosophical Transactions of the Royal Society of London: B. Biological Sciences* **348** (1995), pp. 143–152.

Takahashi et al (1997). T. Takahashi, R.A. Feely, R.F. Weiss, R.H. Wanninkhof, D.W. Chipman, S.C. Sutherland and T.T. Takahashi, Global air–sea flux of CO_2: an estimate based on measurements of sea–air pCO_2 difference. *Proceedings of the National Academy of Sciences of the United States of America* **94** (1997), pp. 8292–8299.

Takahashi et al (2002). Takahashi, T., Sutherland, S.C., Sweeney, C., Poisson, A., Metzl, N., Tilbrook, B., Bates, N., Wanninkhof, R., Feely, R.A., Sabine, C., Olafsson, J., Nojiri, Y., 2002. Global sea–air CO_2 flux based on climatological surface ocean pCO_2, and seasonal biological and temperature effects. Deep-Sea Research II 49, 1601–1622.

Vinnikov et al (1999). K.Y. Vinnikov, A. Robock, R.J. Stouffer, J.E. Walsh, C.L. Parkinson, D.J. Cavalieri, J.F.B. Mitchell, D. Garret and V.F. Zakharov, Global warming and Northern hemisphere sea ice extent. *Science* **286** (1999), pp. 1934–1937.

Wanninkhof (1992). R. Wanninkhof, Relationship between wind speed and gas exchange over the Ocean. *Journal of Geophysical Research* **97** (1992), pp. 7373–7382.

Weiss (1974). R.F. Weiss, Carbon dioxide in water and seawater: the solubility of a nonideal gas. *Marine Chemistry* **2** (1974), pp. 201–215.

Weiss et al (1992). Weiss, R.F., Van Woy, F.A., Salameh, P.K., 1992. Surface water and atmospheric carbon dioxide and nitrous oxide observations by shipboard automated gas chromatography: results from expeditions between 1977 and 1990. Scripps Institution of Oceanography, Reference Series, 92-11, Carbon Dioxide Information Analysis Center, Oak Ridge National Laboratory, ORNL/CDIAC-59, NDP-044, 144pp.